ISSN: 2755-0141

Japan Journal of Clinical & Medical Research

SCIENTIFIC Research and Community

Research Article

Open Access

Computational Prediction of COVID-19 Transmission in Internal Air-Conditioned Environments

Ioannis Rentoumis and NC Markatos*

Computational Fluid Dynamics Unit, School of Chemical Engineering National Technical University of Athens, Greece

ABSTRACT

COVID-19 has had destructive consequences for health, economy and has altered every aspect of everyday human activity. The outbreak was first identified in December 2019 in Wuhan, China. The declaration of the disease as a "Public Health Emergency of International Concern" for the World Health Organization took place on January 30, 2020. Furthermore, 105,5 million cases have been reported until 06 February 2021. Public distancing in internal environments has been applied as a safety measure to prevent transmission. A controversial topic is the safe distance from person to person. The social distancing regulation, for internal public places, has been arbitrarily defined ignoring the potential aerodynamics effects of inlets, such as air-conditioning units, windows and doors. The velocity of the intake airflow has the potential to transfer a droplet from the nose or the mouth of a patient in greater than the indicated distance. The present study focuses on a model of a supermarket that includes a ventilation system and open doors. For the transmission of COVID-19 in an air-conditioned internal space, two different designs were implemented and studied. Internal shelving, furnishing and human models are also being considered. The numerical results obtained are compared with those obtained by two well-known empirical models related to the effective velocity of incoming air and the virus concentration. It is concluded that the computational results obtained in the present study are in acceptable agreement with those obtained by simple empirical models, especially when the standard k-ε model of turbulence is used. Thus, for the cases of coughing and sneezing patients, where we studied the largest particles that sediment onto the floor, the 6-foot (≈1,82 m) rule applies well. However, pathogen-laced particles, coming for example from asymptomatic patients, travel through the air indoors when people breathe and talk. Therefore, there is not much benefit to the 6-foot rule because the air a person is breathing tends to rise and comes down elsewhere, so the person is more exposed to the average background than to a person at a distance. Future research should concentrate rather on the amount of time spent inside rather than distances. As the COVID-19 pandemic is progressing, the present study is flexible and can be applied generally in crowded places. Furthermore, the general outcome is that individuals should maintain the distance of 1,65 meters and it should be applied as guidelines to help reduce the infection risk.

***Corresponding author**

NC Markatos, School of Chemical Engineering, National Technical University of Athens, Greece. Tel: +30210772 3126; E-mail: n.markatos@ntua.gr

Received: December 07, 2022; **Accepted:** December 16, 2022; **Published:** December 23, 2022

Introduction

Even though the transmission rate in China, the country of origin of Covid-19 has been brought down, there are several other countries around the globe that are struggling to contain the disease. Research has shown this disease to transmit through saliva, in the form of small droplets produced by sternutation and coughing [1]. Therefore, there may be airborne infection due to pathogen matter in the form of small particles that disseminate the virus, spreading through large areas as aerosols [2]. Aerosols formed from persons infected with SARS-CoV-2 have the potential, under experimental circumstances, to remain viable and infectious for hours [3]. Even though those tests were conducted at laboratory environments there are enough to demonstrate virus aerosols transmitting potential. To avoid the transmission, social distancing measures have been taken and are in effect, which restrict congestion in public places and define a safe distance from person to person. Although different safe distance measures have been applied around the globe, the most common one is the 1,5 m distance [4]. Thus, it has been shown that most droplets are landing to the ground, or they evaporate before reaching the distance of 1,5 m. Unfortunately, real internal environments that always include doors, windows and various ventilations systems, all of which are altering the aerodynamics characteristics, have not been taken into account. Furthermore, the air-conditioning in most public spaces strongly affects the air-change rate and the temperature stratification in the interior of a building [5].

The purpose of the present work is to test the validity of guidelines given in various countries and to provide a flexible prediction tool for more sophisticated scenarios concerning safe distances among people in public spaces of realistic configurations. The computational tool is demonstrated by applying it to a large air-conditioned supermarket, for two design cases.

The physical problem considered, and modeling assumptions made are presented as follows. From the outbreak of COVID-19, scientists focused most of their efforts to investigate the potential role of aerosols in the transmission of the virus. Similarly, this is the goal of this research while involving the influence of air-conditioning units. A transient CFD simulation is implemented to track the pathway of the exhaled virus concentration during sneezing. The scenario of closed public space has been represented by a supermarket. Shelves, cashier's benches, windows, doors, ventilation on the ceiling, air-conditioning units, etc. have been

designed. Figure 1 depicts the CAD model of a human serving the purpose of the virus carrier.

Two different designs have been implemented. For design 1(Figure 1) the length, breadth and height of the supermarket are 30 m, 25 m and 15 m respectively. Design 1 can be taken as an example for large public spaces due to its extended dimension, it can be also applied to (banks, hospital waiting areas, public services, etc.). A CAD model of a human body which is representing the virus carrier has been placed in a distance of 1,5 meters between a second model. The second human model is placed facing the first.

For design 2(Figure 2) the length, breadth and height of the supermarket are 10 m, 10 m and 4 m respectively. Design 2 is intended to simulate a smaller public place. The second human model in some cases was acting as a blockage. Thus, in design 2 it was removed to calculate the concentration of virus at a distance further than 1,5 m. The person is located 4 m away from the A/C unit. The A/C unit has been placed 2,5 m from the left wall at the x coordinates and 2 m from the floor at the z coordinates. The inlet of the contaminate emissions, which is described as the nose and mouth area of the person while he sneezes, has dimension 5 cm width and 8 cm height.

This study focuses on the airborne transmission/propagation of the particles in ventilated public places, through numerical simulation. The assumptions made for the simulation approach are the following: (a) steady-state simulation of incompressible flow of a Newtonian fluid, (b) adiabatic walls, (c) constant air properties at 298,5 K, (d) the COVID-19 droplets have been modeled in the form of concentration through the air, (e) heat transfer at the walls by either conduction or radiation is neglected, and (f) Neutral atmospheric conditions of the incoming wind.

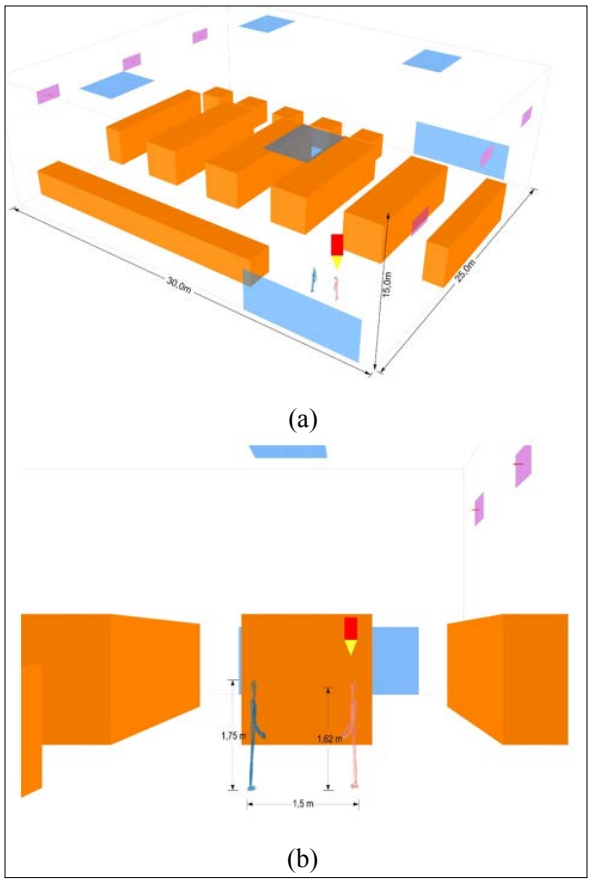

(a)

(b)

Figure 1: Dimension of the design1: (a) overall internal geometry, (b) the human models

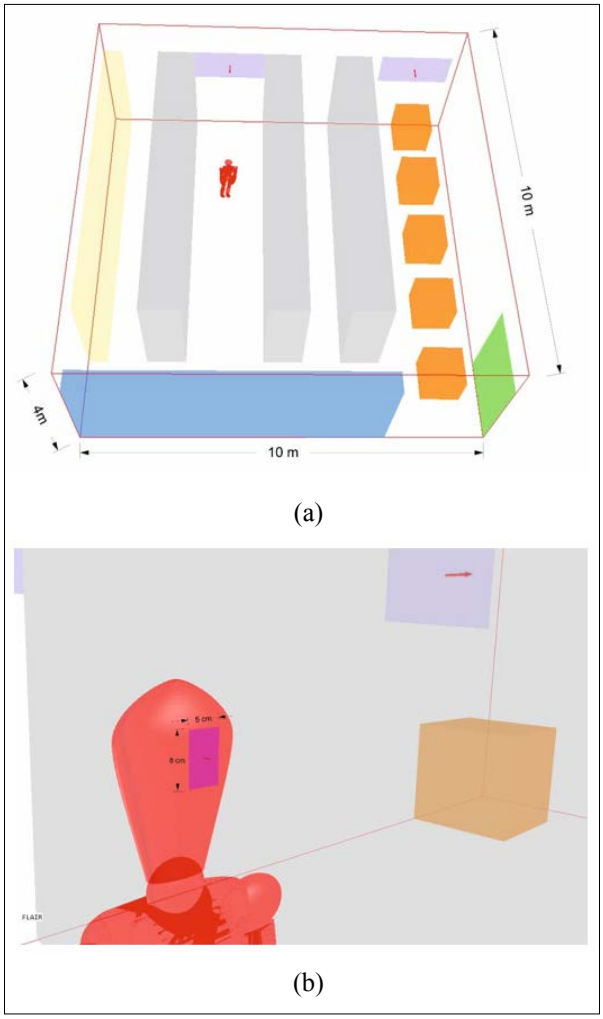

(a)

(b)

Figure 2: Dimension of the design 2: (a) overall internal geometry, (b) the model's facial area

Mathematical modeling

Governing Differential Equations and Turbulence Models

In the steady–state problem, the independent variables are the three components (x, y, z) of a Cartesian coordinate system. The flow can be characterized using the three velocity components (u, v, w), pressure p, enthalpy h, kinetic energy of turbulence k, and the kinetic energy dissipation rate ε.

Apart from pressure, all these dependent variables appear as the subjects of the following general differential equation:

$$\frac{\partial(\rho\varphi)}{\partial t} + div\left(\rho\vec{u}\varphi - \Gamma_{\varphi} grad\,\varphi\right) = S_{\varphi} \qquad (1)$$

where φ: the dependent variable, e.g. velocity components in three space directions (u, v, w), enthalpy (h_e), k and ε, or 1 for the continuity equation.

ρ: Fluid density

$\vec{u}$: Velocity vector

Γ_{φ}: The "effective" exchange coefficient of φ

S_{φ}: Source/Sink rate per unit volume

If flow takes place under steady – state conditions, the general conservation equation (1) for all dependent variables becomes

$$div\left(\rho\vec{u}\varphi - \Gamma_{\varphi} grad\,\varphi\right) = S_{\varphi} \qquad (2)$$

The pressure variable is associated with the continuity equation. This leads to the so-called pressure correction equation, which is deduced from the finite – domain form of the continuity equation. Further details may be found in literature [8]. Several turbulence models were used in the present work, in combination with the Boussinesq approximation for buoyancy effects: The k-ε model, the RNG k-ε model, the Chen-Kim k-ε model and the SST k-ω model, appropriately modified to account for buoyancy forces [6-11]. Use is made of the logarithmic "wall functions" near solid surfaces (11,5 < y+ <150, where y+ is the dimensionless distance of the first grid-node from the wall). Several runs were conducted using different density formulations (density as ideal gas law function of temperature, as an isentropic function and as a Noble-Abel correlation), to test the validity of the Boussinesq approximation. The results show that the validity of the latter is adequate.

Numerical Solution of Equations

To solve the above set of equations a numerical procedure is used based on the Finite Volume Method (FVM) as provided by a general CFD code, i.e., PHOENICS. The basic concept of this method is to discretize the space dimensions (and time also when necessary) into finite intervals and compute the variables correspondingly at only a finite number of points in three – (or four for transient cases) dimensional space. These points are usually called "grid points". The connection between the selected variables is expressed by algebraic equations, derived from their differential counterparts by integration over the control volumes defined by the above-mentioned intervals, in space and time when required, applying the first order upwind scheme for the convective terms and second order central difference scheme for diffusion. More details may be found in literature, e.g. [8,9,13].

Computational Details

The domain of the first design that was modeled has dimensions: X=25m, Y=25m and Z=10,5m and the A/C units were placed at 8 m height. To compare with a smaller domain, design 2 has smaller dimensions: X=10m, Y=10m and Z=4m and the A/C units were placed at 2,5 m height. The distributions of all dependent variables (u, v, w, k, ε, p, T) were calculated throughout that space.

Solution Procedure

The linear equation solver for each finite-volume equation that was used for the present work is a form of Stone's strongly implicit solver without a pre-conditioner [12]. As it is noted in the PHOENICS documentation "TR 006" if the parallel solver option is enabled, as it was in the present's case finer grids, the Stone's solver is replaced by a parallel version of the CGRS solver. The mentioned solvers are included in the CFD package of PHOENICS 2020 and are used without being changed. For convergence criteria the RMS have been set to 1E-4 [13].

Boundary Conditions

A. Inlets

In this problem, there are two types of inlets in both designs. All distances are given at the center of objects. The air-conditioned air is introduced in the supermarket as inlets having a constant velocity of 0,5 m/s. In the first design there are six units placed at the height of 7,5 meters. Three are placed in the plane Ymin and the other three in Ymax at 25 m. The placement at X axis is 4,5, 11 and 17 m and it is the same for the three at the opposite side of the room. In the second design we have 2 units on the same side of the room, placed at 2,5 m in the Z axis and at 3 and 8,5 in the X axis, respectively. The temperature of the cool stream is 14 °C to convey the thermal load of the building. The second inlet was selected to simulate the mouth and nose of a virus contaminated person in a state of sneezing and coughing. Furthermore, the inlet that is describing the mouth and nose has dimensions X=5cm and Y=8 cm. The person releases a spray of virus contaminated droplets (C=1, concentration of COVID-19) at a speed of 4,5 m/s. The temperature at this inlet is 40°C. In the design 1, there is also a healthy person, whose body temperature is 36,6 °C.

B. Outlet

Two doors and four air extraction vents were used as outlets. Moreover, it is assumed that the outlet pressure is equal to the external atmospheric pressure. The air extraction vents are placed on the ceiling of the supermarket.

C Walls

All the walls of the building were defined as adiabatic walls. Furthermore, all the countertops and racks are considered also as adiabatic walls (25 °C).

CPU Time Requirements

The CPU time required for the medium grids of the problem considered to obtain convergence was within 10-14h for the 1.357.752 cells grid of design 2, depending on the different scenarios and the turbulence model used. Computations were performed on a Windows 7 Server (Intel Xeon 2650 v2 8 core, 2,60 GHz CPU and 32GB of RAM)

Results

Spatial Discretization

Design 1

For the numerical solution, a multi-block non-uniform structured grid for each of the two cases is used. The grid is locally refined around the critical area of the two persons. The grid after the refinement around the human model and the mouth and nose is described in the form of Figure 3.

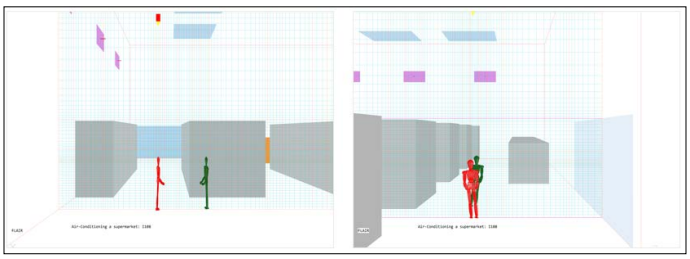

Figure 3: Grid local refinement around human models

Design 2

In this case the computational domain does not contain open windows, and a multi-block non-uniform structured grid, which is locally refined around the human model, is used as well. Details of the grid, after the refinement, is displayed in Figures 4 and 5.

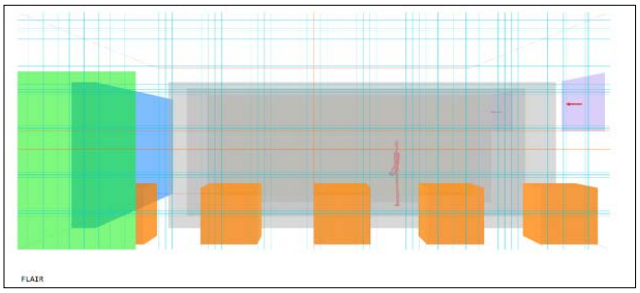

Figure 4: Depiction of the problem's computational grid and the local refinement around the human model (side view)

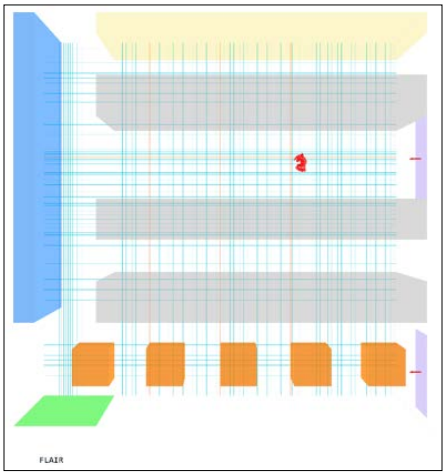

Figure 5: Depiction of the problem's computational grid and the local refinement around the human model (top view)

Grid independency study

Design 1

Grid independence is also tested, by repeating the simulation for a gradually increased grid-cell density. Three grid sizes are tested: the first consisted of 1.301.984 cells, the second consisted of 2.213.120 cells and the third consisted of 2.877.960 cells, those are presented in figure 6.

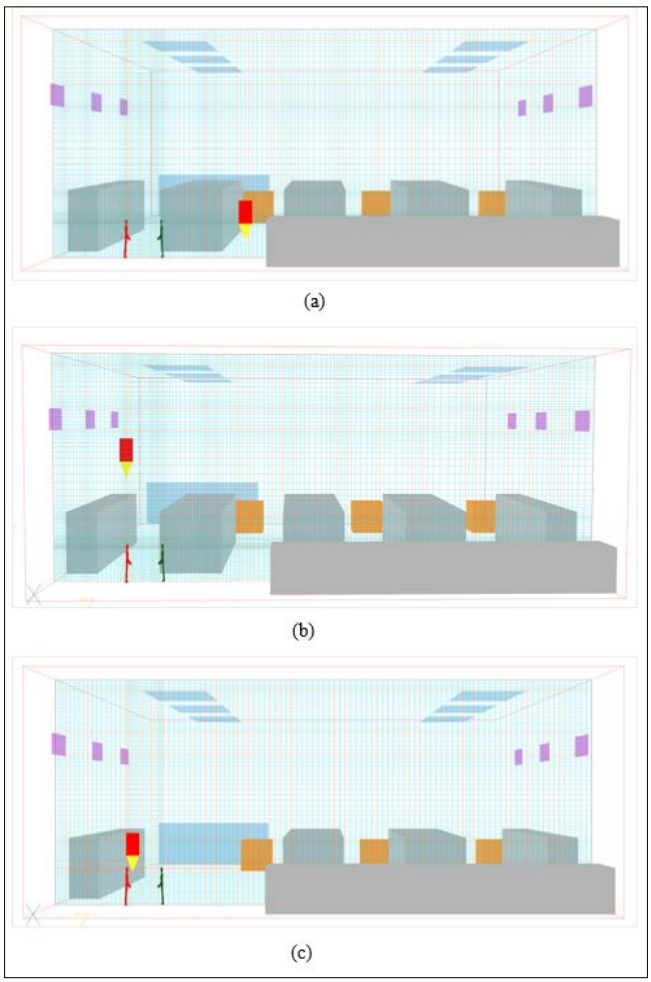

Figure 6: Depiction of the three different grids that are tested, the first consisting of 1.301.984 cells (a), the second of 2.213.120 cells (b) and the third of 2.877.960 cells (c)

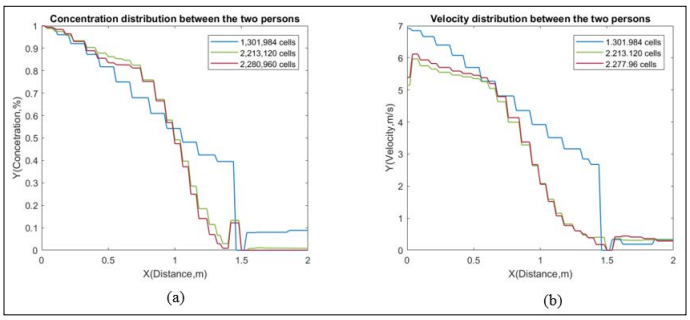

Figure 7: Horizontal distribution of concentration at height Z=1,60m between the two human models, 1.301.984 cells blue, 2.213.120 cells green and 2.877.960 cells purple (a) Concentration (b) Velocity.

Figure 7 presents the concentration percentage at height Z=1,60m between the two human models, as calculated by the three different grids

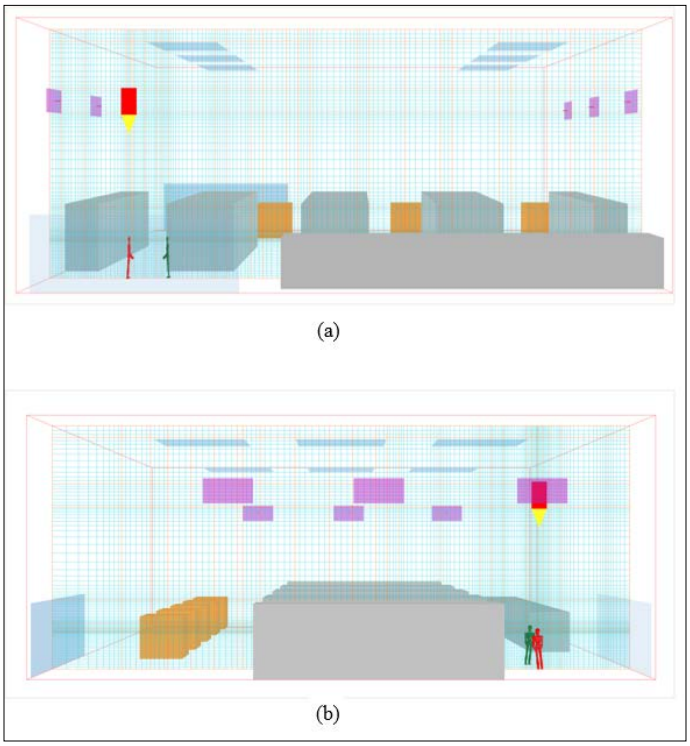

Figure 8: Design 1 spatial discretization: (a) Y-Plane view and (b) X-Plane view

As the value of the data, given by figure 7, comparing the fine and the medium grid are very similar; thus, the medium grid of 2.213.190 cells has been used in design 1 for spatial discretization, which is presented in figures 8.

Design 2

Apart from the standard calculations, grid independence is also tested, by repeating the simulation for a gradually increased grid-cell density. Three different types of grids are tested, of which the coarse one consists of 770.000 cells, the medium one consists of 1.357.752 cells and the fine one consists of 2.047.000 cells. For design 2 the three computational grids that were used are presented in figure 9.

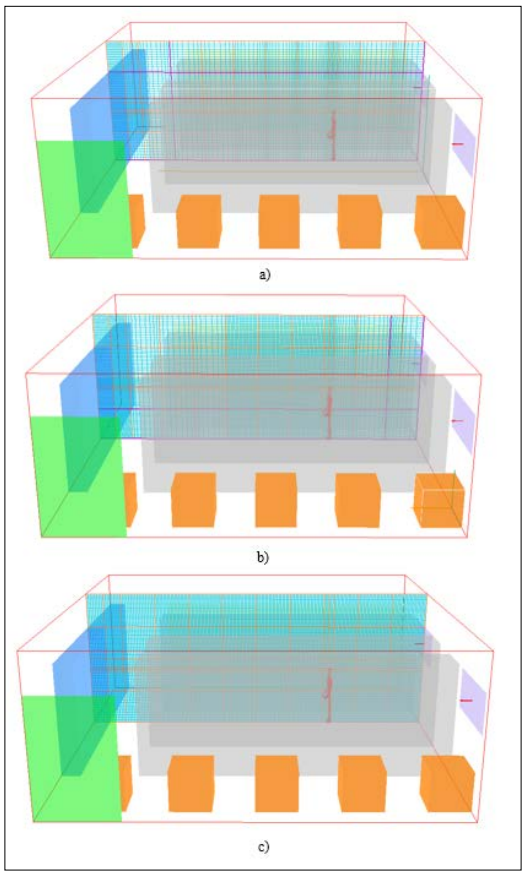

Figure 9: Depiction of the three different grids that are tested, the first consisting of 770.000 cells (a), the second of 1.357.752 cells (b) and the third of 2.047.000 cells (c)

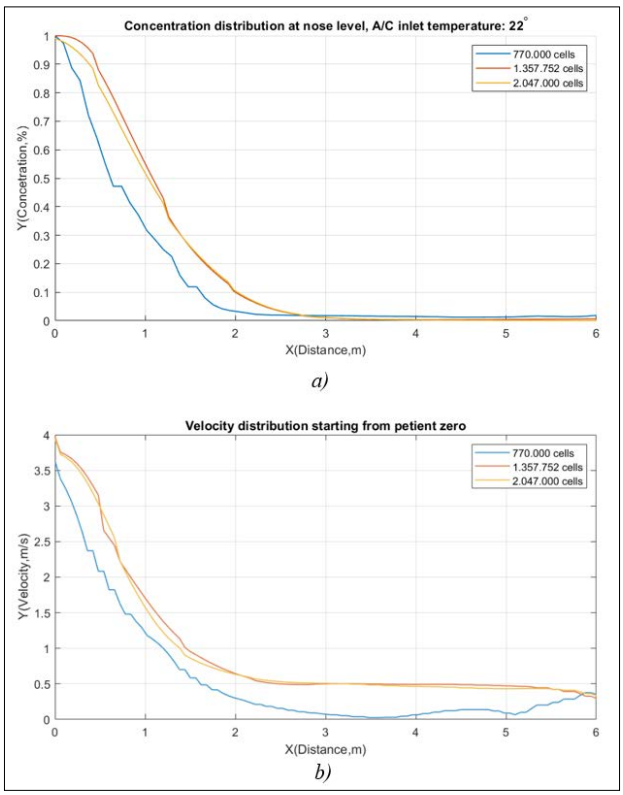

Figure 10: Horizontal distribution of concentration at height Z=1.60m between the two human models 770.000 cells, 1.357.752 cells and 2.047.000 cells (a) Concentration (b) Velocity

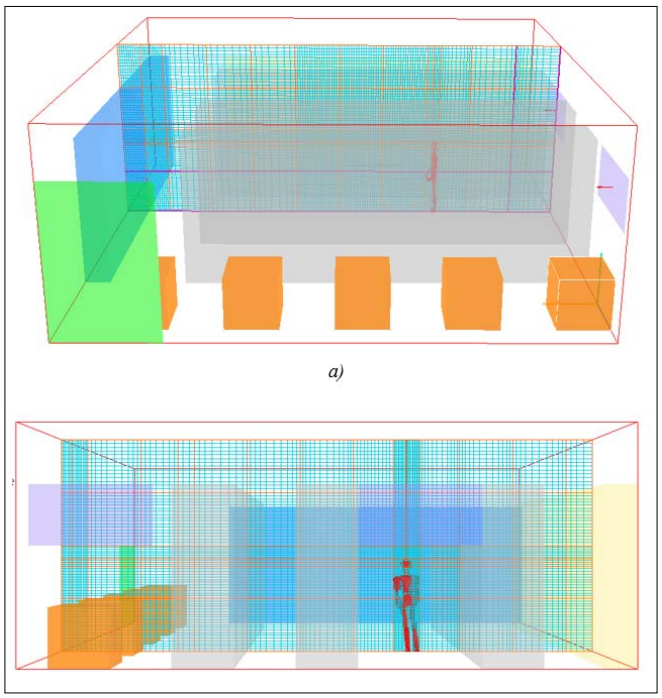

Figure 11: Design 2 spatial discretization: (a) Y-Plane view and (b) X-Plane view

As it is seen in Figure 10, the coarse grid's results for the concentration percentage differ significantly from the results obtained by the other two computational grids. The medium and fine grids, however, yield results of high agreement, which display only a slight divergence at a distance of up to approximately 1,2 meters. Therefore, the medium grid of 1.357.752 cells was used on design 2.

Results of Different Turbulence Models

Design 1

Following a full grid-independence study with all turbulence models, the medium grid was chosen to conduct all ventilation calculations, because the accuracy difference compared with the finest grid was insignificant while the computational cost was not. The turbulence models that were used are the Chen-kim k-ε and the RNG k-ε. In Figure 12, the numerical results obtained by both turbulence models are presented. The start of the X axis is at the location of the mouth and the nose of the virus carrier. Thus, at the start of the X axis the concentration is 1, additionally the concentration value decreases as the distance is increasing [14-19].

In the case of the Chen-Kim k-e the model was able to calculate that the second human model, that is placed opposite to the virus carrier, at 1,5 m is acting as small blockage for the concentration. This is the reason that concentration peaks in that value.

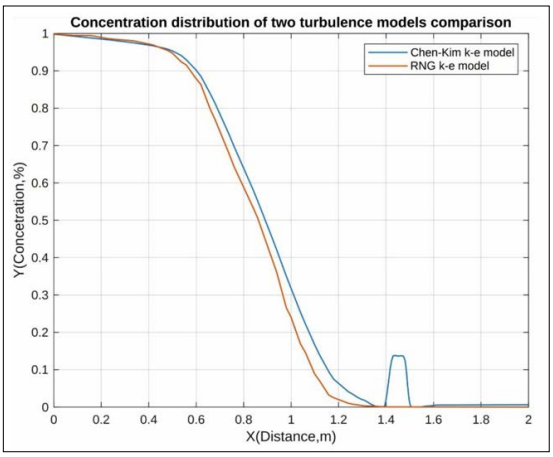

Figure 12: – Concentration distribution: comparison of the two turbulence models prediction (Chen-kim k-e and RNG k-e).

Design 2

As already mentioned, in this case, two different turbulence models were used, in order to perform the calculations: The Chen-Kim k-ε turbulence model and the k-ω SST turbulence model [6,7]. In Figure 14 the results acquired by both of these models are presented.

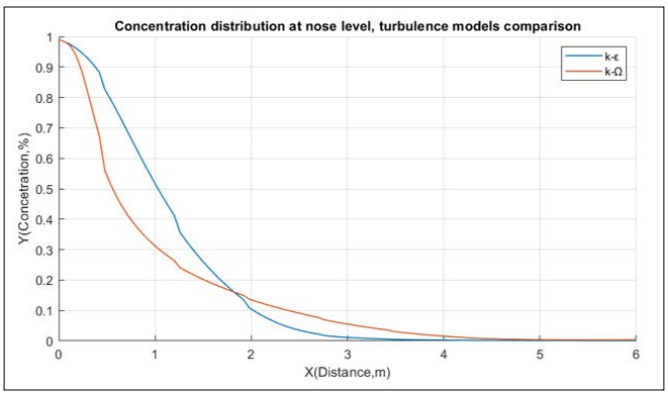

Figure 13: Concentration distribution: comparison of the two turbulence models (Chen-kim *k-ε* and *k-ω SST*)

Parametric Study Results

Design 1

The design 1 parametric study was contacted using the Chen-Kim k-ε turbulence model. Three different scenarios have been studied regarding the temperature and the installation height of the A/C. In the first, the A/C units have been placed at 8 m above the floor and the temperature of the air at the A/C has been set to 14 °C. In the second the height at which the A/C units were placed changed to 4 m, maintaining their temperature, while in the third case the temperature of the units was also changed to 18 °C (table 1).

Table 1: Attributes of the Cases Studied

Attributes/ Case No.	Case 1	Case 2	Case 3
Height of A/C unit (m)	8	4	4
Temperature of the air	14	14	18

The results obtained in the form of concentration percentage, velocity vectors and concentration contours are given in Figures 14-17.

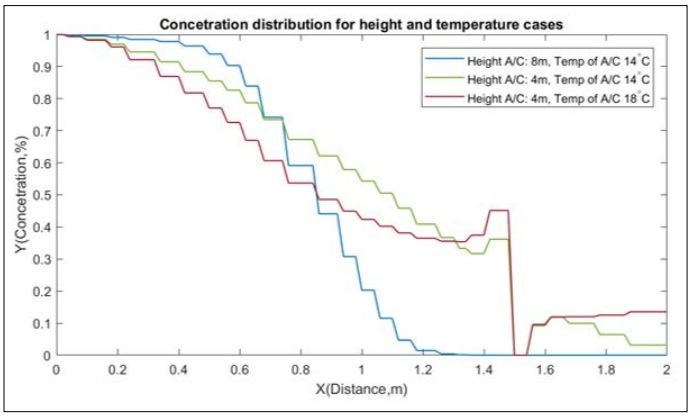

Figure 14: Concentration distribution predicted for the three cases studied

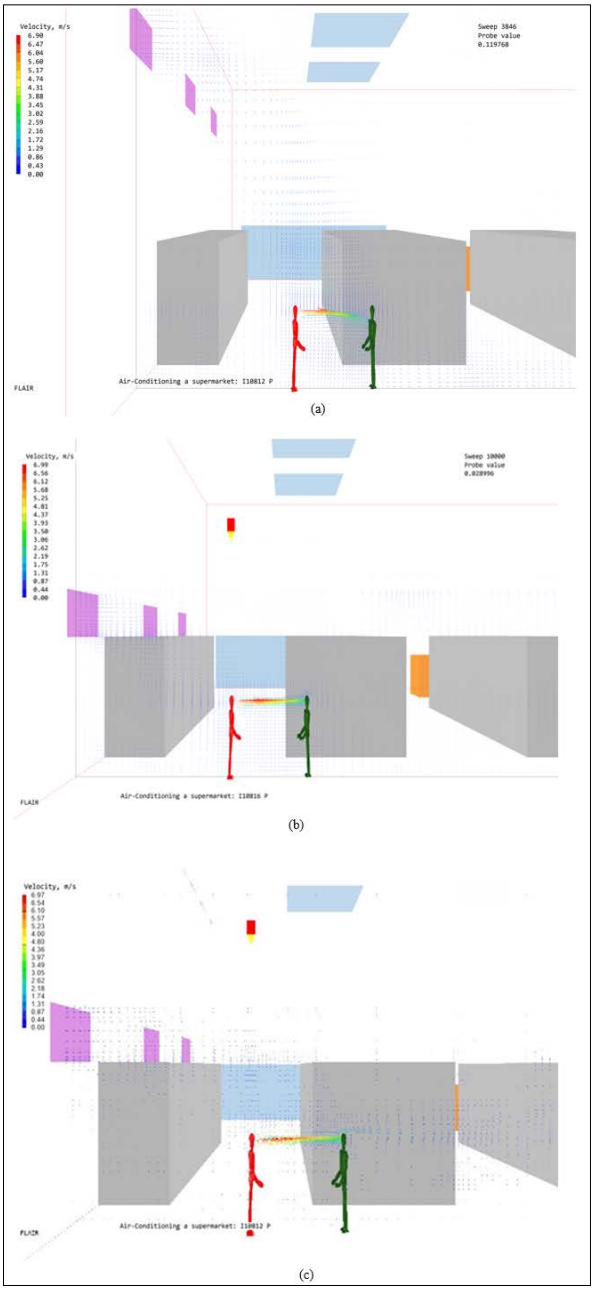

Figure 15: Vectors of velocity in Y-Plane view, (a) Case 1 A/C units at 8 m height and 14 °C, (b) Case 2 A/C units at 4 m height and 14 °C, (c) Case 3 A/C units at 4 m height and 18 °C

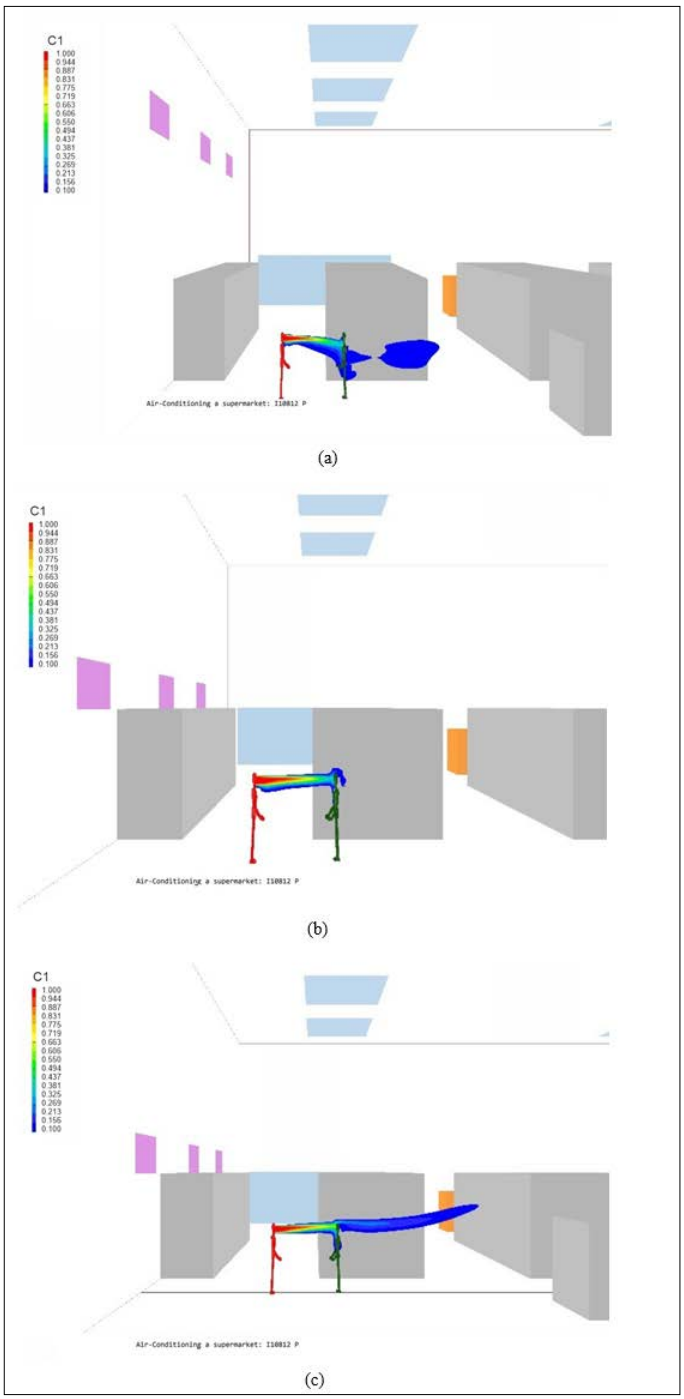

Figure 16: Contour of concentration in Y-Plane view, (a) Case 1 A/C units at 8 m height and 14 °C, (b) Case 2 A/C units at 4 m height and 14 °C, (c) Case 3 A/C units at 4 m height and 18 °C

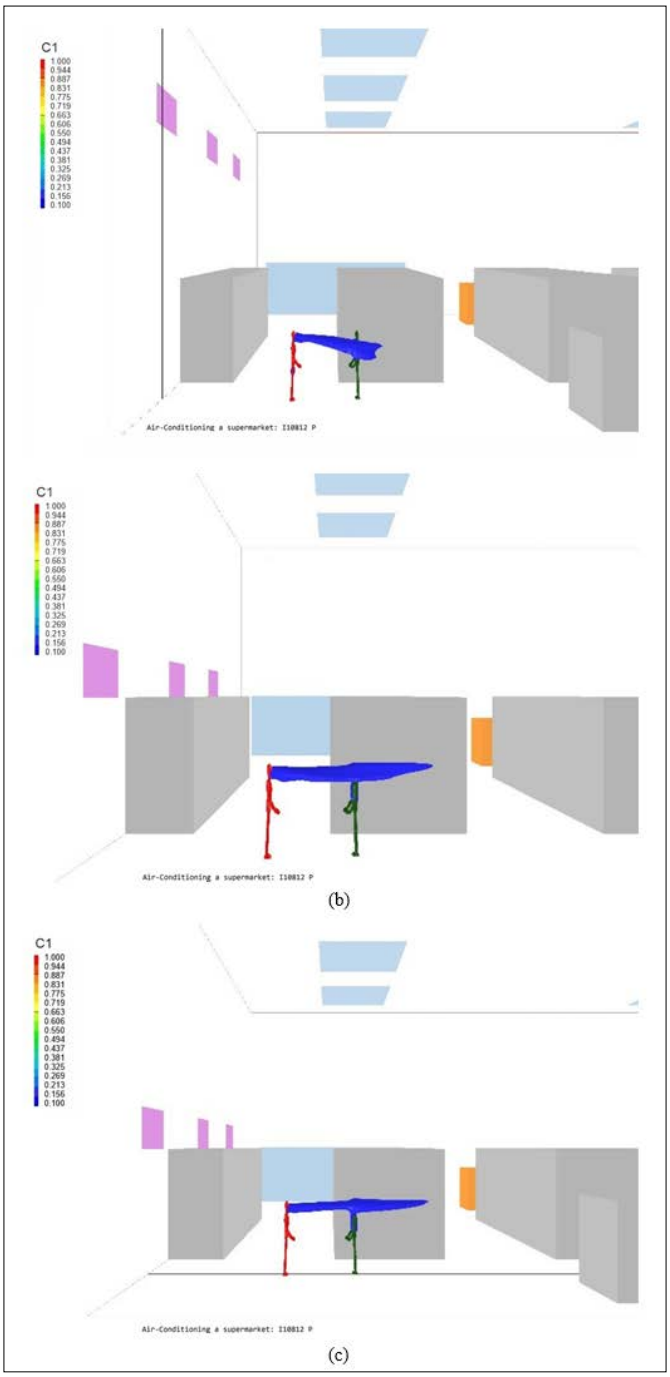

Figure 17: Iso-surface contours of concentration in Y-Plane view, (a) Case 1 A/C units at 8 m height and 14 °C, (b) Case 2 A/C units at 4 m height and 14 °C, (c) Case 3 A/C units at 4 m height and 18 °C

Design 2

For the case in which the air-conditioning air's temperature is higher and equal to 18 °C (in order to ensure that the warmer air does not allow contaminated particles to get entrained towards the floor), the concentration percentage in the X-direction was studied for 3 different cases, which are presented in Table 2. The height, in which the air-conditioning units are placed, is equal to 4 m, in all cases.

Table 2: Attributes of the 3 Cases Studied

Case No.	Case 1	Case 2	Case 3
Air-conditioning inlet velocity (m/s)	0,2	0,4	0,8

In this Design study, only one human model was taken into account, so as to examine how far the virus containing particles are transmitted. The reason for this is that the existence of a second human model complicates this simulation, since it acts as a blockage, thus distorting the concentration's percentage. The results for the Chen-Kim k-ε turbulence model are presented in Figure 18.

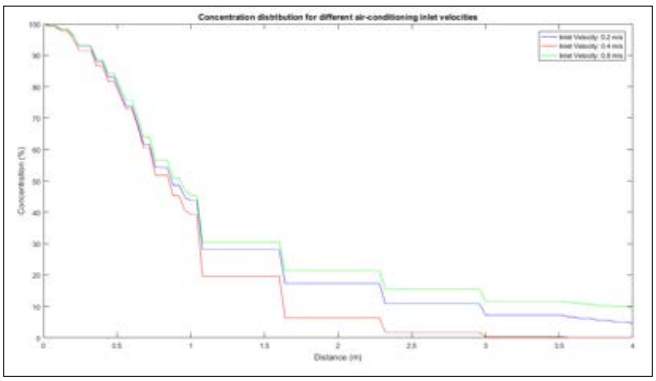

Figure 18: The virus concentration distribution, for the three different cases. The blue line represents an air inlet velocity of 0,2 m/s, the red line represents an air inlet velocity of 0,4 m/s and the green line represents an air inlet velocity of 0,8 m/s

Analysis

Many different runs were performed and generated a lot of data. Due to space restrictions only the most important ones are presented below.

Design 1

From Figure 19, it becomes clear that the virus concentration is quite high, even at a distance of 4 meters from the contaminated person, at least for two of the three air inlet velocities (approximately 5% for an inlet velocity of 0,2 m/s and approximately 10% for an inlet velocity of 0,8 m/s).

It has been found that in the absence of air-conditioning a healthy person has a 17% probability of getting infected at a distance of 1.5 meters from a contaminated person. This probability drops to just 3%, at a distance of 3 meters.

By the results achieved in this case study, it is noticed that the virus concentrations for the three different inlet velocities were calculated as follows

- Inlet velocity of 0,2 m/s: approximately 28,1% at 1,5 m and 10,9% at 3 m
- Inlet velocity of 0,4 m/s: approximately 19,6% at 1,5 m and 0,7% at 3 m
- Inlet velocity of 0,8 m/s: approximately 30,4% at 1,5 m and 12,8% at 3 m

Thus, an inlet velocity of 0,4 m/s is more favorable for the quicker drop of the virus concentration, while also, seemingly, following the non-air-conditioning observations.

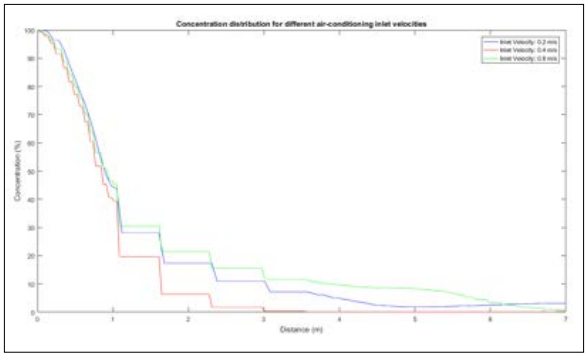

Figure 19: Depiction of the virus concentration distribution, for the three different cases and a distance up to 7 meters

To investigate further the three cases, the concentration's percentage was also plotted up to a distance of 7 meters. The results are shown in Figure 19. For an air inlet velocity of 0,2 m/s, the lowest virus concentration value is marked at approximately 5 meters and is equal to 1,8%, while for an inlet velocity of 0,8 meters, this value is equal to 0,85% and is marked at a distance of 6,9 meters. It is proven once again that the velocity of 0,4 m/s is the most advantageous, since it provides the lowest concentration value of 0,084% at a distance of 5,25 meters.

Calculation of the Virus Concentration Percentage, For Different Air Temperatures

The concentration percentage of the virus was also calculated, for different cases of air-conditioning air temperatures, to comprehend the effect of the air temperature on the way that the contaminated particles get transmitted throughout space.

More specifically, two cases were examined; in the first one, the air temperature is set equal to 18 °C, while, in the second, it is set equal to 20 °C. The distance between the air-conditioning units and the floor remains equal to 4 meters and the inlet velocity of the air is 0,4 m/s.

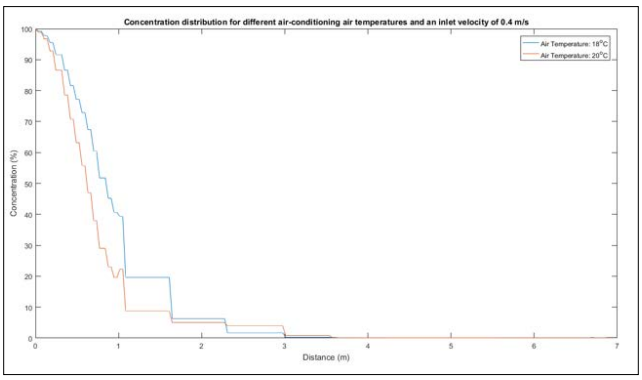

Figure 20: Depiction of the virus concentration, for the two different cases. The blue line represents an air temperature of 18 °C, while the red line represents an air temperature of 20 °C

The results for the Chen-Kim k-ε turbulence model are presented in Figure 20.

Design 2

In the case of a computational domain with closed windows, the effect that the alteration of air-conditioning inlet velocity has on the concentration percentage, is also studied. First, in Figure 21, the concentration percentage in case of absent air-conditioning is presented, while, in Figure 22, the concentration percentage for

different air-conditioning inlet velocities is presented. The results regard the k-ω turbulence model.

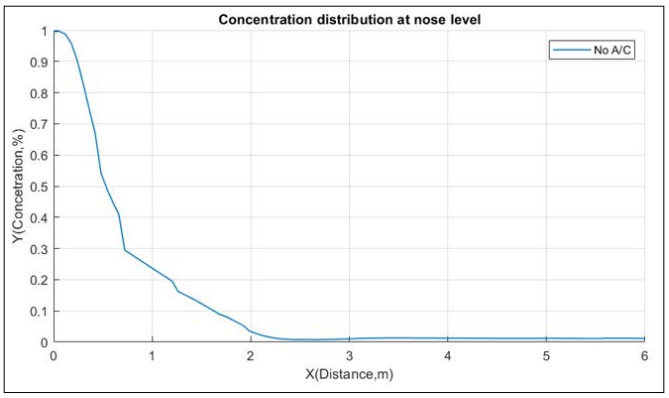

Figure 21: The virus concentration distribution, in case there is no air-conditioning

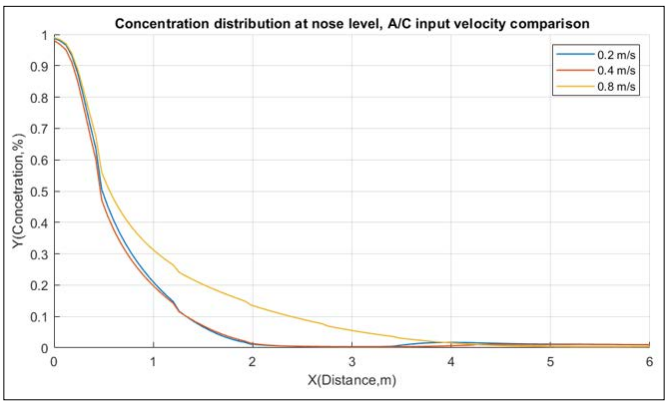

Figure 22: The virus concentration distribution, for three different air-conditioning inlet velocities, namely 0,2 m/s (mild air-conditioning), 0,4 m/s (moderate air-conditioning) and 0,8 m/s (intense air-conditioning)

As expected, for lower air-conditioning inlet velocities (or in the case of absent air-conditioning), the virus does not get transmitted into a big distance, and its concentration diminishes in a faster rate, whereas, for an air-conditioning inlet velocity of 0,8 m/s the virus gets entrained further away, leading to significantly higher concentrations, in the distance range of approximately 0,8 m to 3,5 m. Similar results can be found in literature [20]. This can also be seen in Figures 23 and 24.

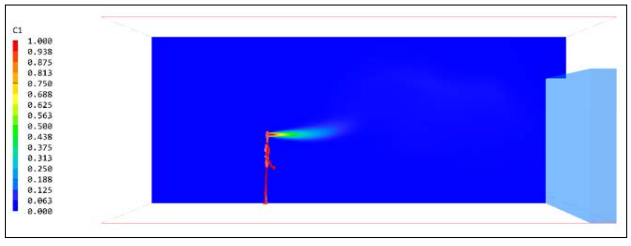

Figure 23: Virus concentration contours (no air-conditioning)

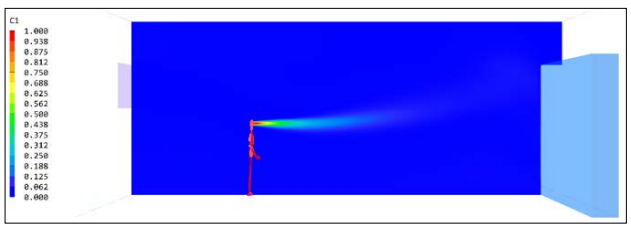

Figure 24: Virus concentration contours (air-conditioning with inlet velocity of 0,8 m/s)

Conclusion

This study provides a quick and easy approach on a CFD calculation of COVID transmission. Thus, it is indeed more simplistic than other relevant studies, although it shares similar and reliable results. A key objective was that simply this general approach can be easily replicated in many other cases. In future time sensitive situations, it can be proven useful due to its flexibility and ease to be converted into different scenarios and produce results fast. As for today a promising start has been made in the vaccination sector and day by day promising treatments are proposed. Even though the progress in pharmaceutical and vaccination is remarkable given the short time, their effectiveness can yet be improved. Furthermore, their supply is still limited. Thus, it is still very important to prevent the transmittance of the virus as much as we can. The virus has been proven very contagious and there is strong evidence that it can be transmitted by inhalation of infected saliva in aerosol particles. Creation of those aerosols is due to breathing, talking, laughing, coughing, or sneezing.

A big step would be to further reduce the infection due to airborne transmission at the lowest possible level and at the same time make the presence of people in public places as sustainable as can be. This investigation was conducted to offer understanding of the airflow patterns in the public places. The goal has been carried out to investigate the transmittance distance of the airborne infectious particles. The current social distancing regulation does not consider possible aerodynamics effects due to A/C, windows, and doors. A ventilated internal space without a mask can be seen as a situation for people that must be strongly avoided. In those cases, the concentration was bigger than 10 % until 3 m and it seems fairly safe only after 6 m. The second design has shown that A/C in its higher operation fan speed enables significantly higher concentration values at the distance between 1 and 3 m. Thus, the high fan operation speed cannot be recommended. Mixed are the results that connect the concentration with the temperature of A/C unit, a firm conclusion cannot be made in those cases. Finally, the case without A/C units has shown less than 10 % after 1,65m that justifies the current regulation that indicates 1,5m for safe distance (with a possibility of 16% to be infected or a 2% at a distance of 3m).

To conclude the guidelines regarding the 1,5 m of social distancing rule that was set in Australia, Belgium, Germany, Greece, Italy, Netherlands, Portugal and Spain are validated by this study. On the contrary China, Denmark, France, Hong Kong, Lithuania and Singapore that set guidelines of 1m are not enough to protect people, in cases of outbreaks. While the 2m that was set in Canada and the UK are overly strict.

References

1. Yang X, Ou C, Yang H, Liu L, Song T, et al. (2020) Transmission of pathogen-laden expiratory droplets in a coach bus. Journal of Hazardous Materials 397: 122609.
2. Jayaweera M, Perera H, Gunawardana B, Manatunge J (2020) Transmission of COVID-19 virus by droplets and aerosols: A critical review on the unresolved dichotomy. Environmental Research 188: 109819.
3. Doremalen N, Bushmaker, Morris D (2020) Aerosol and Surface Stability of SARS-CoV-2 as Com-pared with SARS-CoV-1. The New England Journal of Medicine 382: 1564-1567.
4. Reinders Folmer C, Kuiper ME, Olthuis E, Kooistra EB, de Bruijn AL, et al. (2020) Compliance in the 1.5 meter society: Longitudinal analysis of citizens' adherence to covid-19 mitigation measures in a rep-resentative sample

in the Netherlands. SSRN Electronic Journal DOI: 10.2139/ssrn.3624959.

5. Patel A, Dhakar P (2018) CFD Analysis of Air Conditioning in Room Using Ansys Fluent. JETIR 5.
6. Wilcox DC (2008) Formulation of the K-W turbulence model revisited. AIAA Journal 46: 2823-2838.
7. Prandtl L (1925) "Z. angew". Math. Mech 5: 136-139.
8. Versteeg HK, Malalasekera W (2007) An Introduction to Computational Fluid Dynamics: The Finite Volume Method. Pearson Education Limited.
9. Yakhot V, Orszag SA, Thangam S, Gatski TB, Speziale CG (1992) Development of turbulence models for shear flows by a double expansion technique. Physics of Fluids A: Fluid Dynamics 4: 1510-1520.
10. YS Chen, SW Kim (1987) Computation of turbulent flows using an extended k-e turbulence closure model. NASA CR-179204.
11. Lee D, Yeh CL (1993) Computation of reacting flame stabilizer flows using a zonal grid method. Nu-merical Heat Transfer, Part A: Applications 24: 273-285.
12. Stone HL (1968) "Iterative Solution of Implicit Approximations of Multidimensional Partial Differential Equations". SIAM Journal on Numerical Analysis 5: 530-538.
13. Saad Y, Jocelyne E (1998) A deflated version of the Conjugate Gradient Algorithm. SIAM Journal on Scientific Computing 21: 1909-1926
14. Y.S.Chen and S.W.Kim, 'Computation of turbulent flows using an extended k-e turbulence closure model', NASA CR-179204, (1987).
15. DJ Monson, HL Seegmiller, PK McConnaughey, YS Chen (1990) 'Comparison of experiment with cal-culations using curvature- corrected zero and two-equation turbulence models for a two- dimensional U-duct', AIAA 90-1484.
16. J O Hinze (1959) 'Turbulence', McGraw Hill Book Company, Chapter 3: 181-190.
17. LM Smith, WC Reynolds (1992) 'On the Yakhot-Orszag Renormalization group method for deriving turbulence statistics and models', Phys. Fluids A 4: 364.
18. V Yakhot, SA Orszag (1986) 'Renormalization group analysis of turbulence', J.Sci.Comput 1.
19. V Yakhot, SA Orszag, S Thangam, TB Gatski, CG Speziale (1992) 'Development of turbulence models for shear flows by a double expansion technique', Phys.Fluids A 4.
20. Mortazavy beni, H.; Hassani, K.; Khorramymehr, S. In silico investigation of sneezing in a full real human upper airway using computational fluid dynamics method. Computer Methods and Programs in Biomedicine 2019, 177, 203-209 DOI: 10.1016/j.cmpb.2019.05.031.